

Full Length Research Paper

Constitutive activation of AMP-activated protein kinase (AMPK) propel mitochondrial biogenesis

Paul B. Bokko^{1,2*}, Afsar U. Ahmed^{1,3} and Paul R. Fisher¹

¹School of Life Sciences, La Trobe University, Bundoora, VIC 3086, Australia.

²Department of Veterinary Surgery and Theriogenology, University of Maiduguri, PMB 1069, Nigeria.

³Monash Medical Research Institute, Monash University, Clayton, VIC 3800 Australia.

Received 3 August, 2014; Accepted 19 September, 2014

Mitochondrial biogenesis is primarily a critical adaptation aimed to balance an increased workload in an attempt to maintain appropriate body perfusion. Until recently, the signaling mechanisms responsible for this response are poorly understood. To examine the role of AMP-activated protein kinase (AMPK), an evolutionarily conserved fuel sensor, in mitochondrial biogenesis, we used constitutively active and antisense inhibition genetic tools in *Dictyostelium discoideum*. Constitutive activation of AMPK culminated in mitochondrial proliferation and elevated ATP generation; this became marked with higher plasmid copies. Antisense inhibition of AMPK yielded non-significant decrease in the mitochondrial content at low levels. However, the more severe the antisense inhibition, the more significant the diminution of AMPK function, resulting in the more apparent decrease in the Advanced Technology Program (ATP) and mitotracker fluorescence. This finding provides direct genetic evidence that AMPK plays a significant role in ameliorating the effects of cellular energy deficit through mitochondrial proliferation. Thus, the constitutive activation of AMPK initiates signalling to downstream targets. The result perturbation of these pathways would culminate in the mitochondrial biogenesis. Taken together, these findings show the constitutive activation of AMPK propels *in vivo* mitochondrial biogenesis and ATP generation in *D. discoideum* as in other organisms.

Key words: Antisense, constitutive activation, *Dictyostelium discoideum*, mitochondrial mass, plasmid copies.

INTRODUCTION

Mitochondrial biogenesis is a critical adaptation to chronic energy deprivation such as chronic metabolic stress and long-term exercise, rather than in phase with the cell cycle (Zong et al., 2002; Ventura et al., 2008). During increased energy demands, imbalance between rates of adenosine triphosphate (ATP) synthesis and consumption

in the mitochondria would lead to a deleterious drop in energy-rich phosphate compounds (Goffart et al., 2004). Moreover, the primary indicator of altered energy production in the cytosol is the [ATP]/[ADP]/[Pi] ratio (Hardie and Hawley, 2001). The problem may even be aggravated if there are defects in mitochondrial function

*Corresponding author. E-mail: bokkopx@yahoo.com.

Author(s) agree that this article remain permanently open access under the terms of the [creative commons attribution license 4.0 international license](http://creativecommons.org/licenses/by/4.0/)

itself (Bokko et al., 2007). The energy depletion becomes physiologically notable especially during high workload, and this leads to the induction of compensatory reactions and adaptations that result in an increase in the maximal capacity to generate ATP (Wakerhage and Woods, 2002). The accuracy of mitochondrial biogenesis relies on the spatiotemporally coordinated synthesis, import and correct assembly of about 1,100 nuclear encoded proteins (Ventura et al., 2008; Scarpulla et al., 2012). The precursor proteins are escorted by molecular chaperones, imported and refolded into intramitochondrial proteins and to specific mitochondrial compartments (Hermann and Neupert, 2000). Other proteins encoded by mitochondrial DNA (mtDNA) necessary for the components of the electron transport chain, mitochondrial replication, fusion and fission must also be tightly synchronized to ensure proper mitochondrial function and shape; while striving to meet tissue energy requirements (Ventura et al., 2008). The ability to replicate enables proper organization of the mitochondrial network during biogenesis (Hermann et al., 1998; Chan, 2006). Thus, mitochondrial biogenesis is accompanied by variations in mitochondrial size, number and mass (Ventura et al., 2008; Scarpulla et al., 2012). Conversely, mitochondria can also undergo fusion or become inactive when energy use is low (Hermann et al., 1998; Chan, 2006).

Recent advances in molecular biology have started to elucidate the transcriptional events governing mitochondrial biogenesis. For instance, acute activation of AMPK in muscle helps defend against energy deficiency by promoting increased glucose transport and fatty acid oxidation through increased GLUT4 translocation (Ihleman et al., 1999; Hayashi et al., 2000; Bergeron et al., 2001). Prolonged AMPK activation coordinately triggers cell adaptation to energy stress by translating diverse physiological/metabolic perturbations into an increased capacity to generate energy via the expression of key transcriptional regulator genes of mitochondrial biogenesis (Bergeron et al., 2001). A particular significance is the expression of the peroxisome proliferator-activated receptor- γ (PPAR- γ) coactivator 1 α (PGC-1 α)/PPAR α (Puigserver et al., 1998; Wu et al., 1999; Lin et al., 2002; Goffart et al., 2004) and calcium/calmodulin-dependent protein kinase IV (CaMK IV) (both master regulators of mitochondrial biogenesis) (Hawley et al., 1995; Wu et al., 2002).

Coactivation of PGC-1 α and nuclear respiratory factors (NRF-1 and NRF-2) cause the induction of the mitochondrial transcription factor A (mTFA) (Puigserver et al., 1998; Wu et al., 1999; Lin et al., 2002). The mTFA in turn upregulates the expression of nuclear and mitochondrial genes encoding mitochondrial proteins (Gulick et al., 1994; Wu et al., 1999; Bergeron et al., 2001; Lehman and Kelly, 2002; Vega et al., 2000). The outcome is transcription and replication of key mitochondrial enzymes

(Clayton, 1992; Winder et al., 2000), mitochondrial biogenesis to increase mitochondrial oxidative capacity (Williams et al., 1986; Zong et al., 2002) and ATP generation (Xia et al., 1997; Bergeron et al., 2001). Expression of PGC-1 α in C2C13 myoblasts cells (Wu et al., 1999), the heart (Lehman et al., 2000; Michael et al., 2001; Lehman and Kelly, 2002; Suzuki et al., 2007) and in skeletal muscle of transgenic mice stimulates mitochondrial biogenesis leading to a dramatic increase of mitochondrial mass and size in neonatal mice and mitogenesis in adult mice (Michael et al., 2001; Lin et al., 2002). The action of PGC-1 α in turn is controlled by the coordinated actions of myocyte enhancer factor-2 (MEF2) transcription factor and class II histone deacetylases (HDACs) regulatory pathway via two MEF2-binding sites on the upstream/promoter region of PGC-1 α (McKinsey et al., 2001; Czubryt et al., 2003; Black and Olson, 1998). The MEF2 through PGC-1 α drive mitochondrial enzyme expression, growth and mitochondrial energy production (Czubryt et al., 2003). Prolonged MEF2 function activates HDACs, thereby negatively regulating the expression of PGC-1 α (Grozinger and Schreiber, 2000; McKinsey et al., 2001). Conversely, inactivation of HDACs kinases derepresses PGC-1 α expression, resulting in increased mitochondrial biogenesis (Czubryt et al., 2003).

Furthermore, chronic administration into nonexercising muscles of β -guanidinopropionic acid (GPA) (depletes phosphocreatine and ATP) (Bergeron et al., 2001) or 5 - aminoimidazole-4-carboxamide-1- β -d-ribofuranoside (AICAR) (Corton et al., 1995; Reznick and Shulman, 2006) or metformin (Liu et al., 2006) increases the expression of CaMK IV and PGC-1 α in skeletal muscle (Bergeron et al., 2001; Zong et al., 2002). In addition, NRF-1 binding activity, δ -ALAS mRNA expression, cytochrome c protein expression, key mitochondrial enzymes and mitochondrial content are also upregulated. Conversely, GPA treatment of transgenic mice expressing dominant-negative mutant of AMPK expression (DN-AMPK) in muscle did not induce the expression of signaling molecules/pathways like the PGC-1 α and CaMK IV or exhibit mitochondrial biogenesis (Woods et al., 2000; Zong et al., 2002). Recently, expression of endothelial nitric oxide synthase (eNOS) increased mitochondrial DNA content, cytochrome c and cytochrome c-oxidase IV protein expression levels, and PGC-1 α , NRF-1, and mtTFA mRNA expression (Nisoli et al., 2003), and consequently, mitochondrial biogenesis.

Though, it has been known for decades that physical activity is associated with increased mitochondrial content, it is only known recently that some of the critical factors involved in the regulation of mitochondrial biogenesis have been identified. AMPK is an attractive potential candidate, and its role in this process has been advocated by recent correlative studies demonstrating that AMPK activation is associated with increased

mitochondrial enzyme content (Winder et al., 2000) and mitochondrial biogenesis in rats (Bergeron et al., 2001). In earlier report, AMPK phenocopied mitochondrial dysfunction and signal transduction dose dependently. Given AMPK functions as key regulator of energy metabolism, the study centred on assessment of its role in mitochondrial biogenesis. Here we report that constitutive activation of AMPK propel mitochondrial biogenesis in *Dictyostelium discoideum*.

MATERIALS AND METHODS

Many molecular biological techniques were used as described by Ausubel et al. (1995). Sequence analyses, alignments and database searches were conducted using web-based software through dictyBase (<http://www.dictybase.org/blast>), ExpASY (Expert Protein Analysis System) site (<http://www.expasy.org>) and at the Australian Genome Research Facility (www.agrf.org.au).

Dictyostelium discoideum: Strains and culture conditions

All experiments were conducted with *D. discoideum* strain AX2 (Watts and Ashworth, 1970) and strains derived from it (Bokko et al., 2007). Each strain carried multiple copies of the following plasmids: (1) pPROF362 (AMPK α subunit antisense inhibition construct) in HPF456 to 462; (2) pPROF361 (corresponding RNA control construct) in HPF466 to 468; or (3) pPROF 392 (AMPK α^{380} overexpression construct) in HPF434 to 442 strains. All strains were isolated using the Ca(PO₄)₂/DNA coprecipitation method (Nellen et al., 1984) and selected as isolated, independent colonies on *Micrococcus luteus* lawns on standard medium (SM) agar supplemented with 20 μ g/ml geneticin (G-418) (Promega Corporation, Madison, WI). Cells were cultured in axenic medium (HL-5) supplemented with 100 μ g/ml ampicillin and 20 μ g/ml streptomycin or on *Klebsiella aerogenes* lawns on SM agar. The selective agent geneticin (20 μ g/ml) was added to HL5 medium for all strains.

Gene cloning and sequence analysis

AMPK cloning strategies and vectors were as described previously (Bokko et al., 2007). The 2.6 kb *snfA* gene (Sung et al., 1999; EMBL/GenBank ID AF118151) encoding the AMPK α subunit was amplified from genomic DNA template using the gene-specific primers PAMKF1 (5'-TCTAGATTTCGAAAAATCATGAGTCCATATCAACAATAATCCCAAT-3') and PAMKR1 (5'-TCTAGACTCGAGTTAACTACAAATATCAAAAATATGAATATTTTACC-3') and cloned into pZerO2 (Invitrogen, Carlsbad, CA) to yield pPROF348 plasmid.

Generation of constitutively active form of AMPK α subunit

The cDNA encoding the catalytic domain of AMPK α subunit was amplified using PACDNF1 (5'-CTCGAGTTTCGAAATGAGTCCATATCAACAAAATCCCATTGG-3') and PACDNAR1A (5'-CTCGAGAATTCTTATTGGCTCTGGGGAGCACTGACAT-3') primers by reverse transcription PCR (RT-PCR) using RNA template extracted from AX2 cells using RNazol (Life Technologies

Inc., Grand Island, NY). The amplified catalytic domain comprising 1140 bp cDNA fragment designated AMPK α^{380} was cloned into pZerOTM-2 thereafter, subcloned into the *Clal* – *XhoI* sites of the pA15GFP (Fey et al., 1995), replacing the resident green fluorescent protein (GFP) gene, creating a fusion of the actin15 promoter-AMPK gene to yield pPROF 392 for overexpression of a constitutively active, truncated AMPK α subunit.

Creation of the AMPK α subunit antisense/sense constructs

Antisense inhibition offers partial inhibition of expression of essential genes producing sublethal phenotypes. Plasmid constructs for expression of antisense RNA and the corresponding sense RNA control were created from pPROF348 template by amplifying a fragment using primers PAMPKF10 (5'-TCTAGAATTCCTATGGATGAAAAGATTAGAAGA-3') and PAMPKR10 (5'-TCTAGAATTCCTCATGCTATTGCTATTGGTGG-3'), cloned into *XbaI* site of pZerOTM-2. The DNA fragment(s) were subcloned into the *EcoRI* site of the *Dictyostelium* expression vector, pDNeo2 (Witke et al., 1987) in either orientations. The result of AMPK α subunit sense (pPROF361) and antisense (pPROF362) plasmid express 1172 bp of the AMPK α antisense RNA or the corresponding sense RNA control. Both fragments would be expressed under the control of the *Dictyostelium* actin 6 promoter. AMPK α subunit DNA fragments cloned into appropriate plasmids were submitted to the Australian Genome Research Facility (AGRF), Brisbane, Australia for sequencing.

Determination of plasmid copies in strains

The plasmid copies in the various strains were determined by Southern blotting using enhanced chemifluorescence measurements in a fluorimager (Storm860TM) (Amersham Biosciences, Castle Hill, Sydney, Australia). Genomic DNA preps were extracted from AX2 and from each strain. Each strain was digested with *EcoRI*, separated by gel electrophoresis, blotted onto nylon membrane and probed with fluorescein-labelled AMPK α subunit DNA as well as G β -protein DNA probe(s) in combination with antifluorescein alkaline peroxidase-conjugated antibody. The plasmid copies were quantitated using the ImageQuant tools (TLv2003.03) program; computed as the ratio of the RFU values of respective strain to the RFU values of AX2.

Estimation of RNA expression in strains

RNA was extracted from each strain bearing plasmid vector expressing the catalytic domain of the AMPK α subunit (α^{380}) (pPROF392) or an antisense/sense RNA complementary as part of the catalytic domain of the AMPK α subunit (pPROF362/pPROF361). Northern blotting analysis was performed by blotting nucleic acids onto nylon membrane and probed with DIG-labelled AMPK α subunit DNA probe to determine RNA expression levels in the strains.

Mitochondrial mass by fluorescence microscopy using MitoTracker green or red

Mitochondrial mass was evaluated to investigate mitochondrial biogenesis. Mitochondrial "mass" was measured by fluorescence microscopy after staining the mitochondria with Mito tracker green (a) or Mito tracker red (b) to assess mitochondrial proliferation. (A)

Axentially growing cells at the exponential phase were harvested by centrifugation at $3,000 \times g$ for 15 s, washed once in Lo-Flo HL5 (3.85 g/L glucose, 1.78 g/L proteose peptone, 0.45 g/L yeast extract, 0.485 g/L KH_2PO_4 and 1.2 g/L $\text{Na}_2\text{HPO}_4 \cdot 12\text{H}_2\text{O}$; filter sterile), incubated in Lo-Flo medium for 2 h and then divided into two aliquots. One aliquot was resuspended in Lo-Flo HL-5 containing 200 nm MitoTracker Green FM (Invitrogen), whereas the other aliquot, resuspended in only Lo-Flo HL5 as an unstained control. Both aliquots were incubated for an hour in the dark and then unbound MitoTracker Green was removed by washing the cells three times in Lo-Flo HL5, with 10 min shaking on an orbital shaker (150 rpm) between washes. Finally, the cells were resuspended in Lo-Flo HL5 and fluorescence was measured using the Blue Module in a fluorometer (Turner Biosystems Modulus™). The MitoTracker Green fluorescence per million cells was calculated after subtraction of the background fluorescence in the unstained cells. (B) Cells grown to log phase in HL5 medium were placed on sterile coverslips in six-well plates (Nalge Nunc™, Naperville, IL), washed gently in Lo-Flo HL5 and stained with 200 nm MitoTracker Red CMX-Ros (Invitrogen™) in Lo-Flo HL5 for 1 h in the dark. Unbound MitoTracker Red was removed by washing the cells 3 to 4 times in LoFlo HL5 over 2 h. After two washes in phosphate buffer (12 mm Na_2HPO_4 , 12 mm NaH_2PO_4 , pH 6.5), the cells were fixed and flattened at the same time by placing the coverslips up side down on a layer of 1% agarose in phosphate buffer containing 3.7% paraformaldehyde for 30 min. The fixed cells on the coverslips were washed four times (5 min each) in phosphate-buffered saline and mounted for microscopy. Images of cells and mitochondrial concentrations were obtained and analysed by fluorescence microscopy.

ATP assays

The ATP levels in cells of the AMPK α^{380} overexpressing cells and AMPK antisense-inhibited cells were measured. ATP assays were conducted using the luciferase-based ATP Determination Kit (Biaffin GmbH, Germany) in cells grown axentially in HL5 medium. Background luminescences measured before the assay were subtracted, and ATP concentrations were determined from a standard curve constructed using 10-fold serial dilutions of the ATP standard (1×10^{-7} M to 1×10^{-11} M) in assay buffer.

RESULTS

The AMPK α subunit in *Dictyostelium* is encoded by a 2.6 kb gene annotated as Q9XYP6 (www.expasy.org), AF118151 (www.ncbi.nlm.nih.gov/entrez) and DDB0215396 (<http://www.dictybase.org/blast>); comprised of five exons and four introns. The N-terminus holds a highly conserved catalytic core, S_TKc domain and identical APE and DFG motifs with other eukaryotic cells (Figure 1). It also has asparagine rich C-terminus.

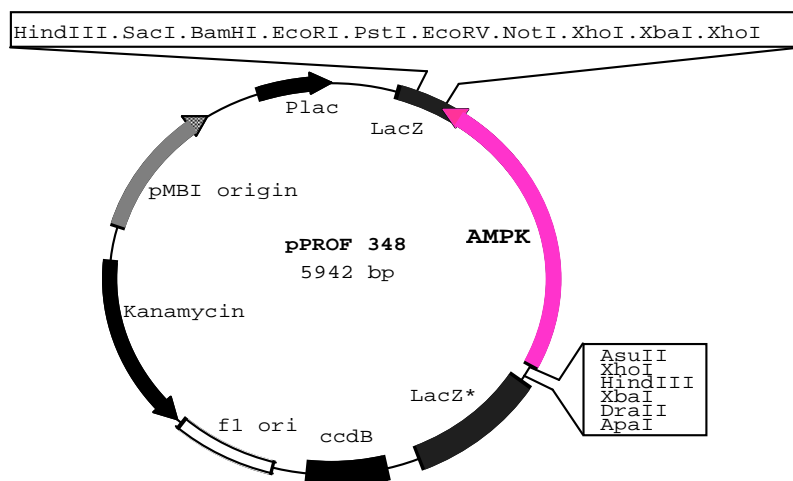
Plasmid copies and RNA expression

The form of the AMPK α subunit that was overexpressed contained the entire catalytic domain but was truncated within the putative region responsible for autoinhibition and binding to the β subunit. The truncation of the AMPK

α subunit in the catalytic domain created a constitutively active form of AMPK. Southern blot analysis for the strains overexpressing truncated AMPK α subunit and strains in which AMPK is antisense inhibited yielded bands that varied in their intensities (Figures 2A and 3A). This indicates different plasmid copies of the respective strains. The least prominent band showed intensity higher than AX2, the wild type strain (Figures 2 and 3). The strains exhibited a characteristic, stable level of RNA expression and the differences reflected the expression plasmid copies in the genome (Figures 2B and 3B). Both plasmid constructs affected expression in a copy number-dependent manner. A steady state level of AMPK α^{380} mRNA in quantitative northern blots tightly correlated with the plasmid copies of the AMPK α^{380} expression construct insertions in the strain genomes (Figures 2A). Overexpression mutants showed strong RNA expression signals of increasing intensities as a number of AMPK α^{380} construct increased (Figure 2). The sense RNA (control) also showed high RNA expression that tightly correlated with the plasmid copies (Figure 3B). By comparison with the sense RNA controls, the equivalent antisense RNA levels were dramatically reduced even at the lowest plasmid copies of the antisense plasmid construct (Figure 3). Interestingly, the extent of RNA reduction correlated with the plasmid copies of the antisense RNA-expression construct (Figure 3). This indicates degradation in the antisense RNA expressing transformants of both the antisense and the native mRNA. This would mean lower expression levels of the native mRNA. Accordingly, the plasmid copies of the corresponding constructs were used as AMPK α subunit expression index. To facilitate analysis and presentation of the data, positive values were assigned to plasmid copies for overexpression constructs while negative values for the AMPK α antisense construct.

Mitochondrial mass

Overexpression of the AMPK α catalytic domain resulted in a strong Mitotracker Green fluorescence per cell, whereas AMPK α antisense inhibition exhibited slight reduction of the fluorescence signal compared to that of AX2 cells (Figure 4). Additionally, there was 2 to 3 fold increase in mitochondrial mass in strains overexpressing AMPK α subunit compared to AX2. Examination of MitoTracker Red stain showed increased mitochondrial fluorescence in AMPK α^{380} overexpression strains but decreased in AMPK α subunit antisense strains compared to AX2 (Figure 5). Increased intensity of MitoTracker Red stain in AMPK α^{380} strains signify elevated mitochondrial mass per cell. The higher the plasmid copies in the constitutively active AMPK strain the more the fluorescence from the assayed cells (Figures 4 and 5). The increase in



(A)

Q9XYP6	Q9XYP6_DICDI	-----MSPYQQNP	IGSLGGLYSGGGIEKSSQI	IGNYRLDK	TLGIGSF	FGK	44
Q38997	KIN10_ARATH	DEFNLVSS	IDHRIFKSRMDGSGT	TSRSGVES	ILPNYKLGR	TLGIGSFGR	55
P54645	AAPK1_RAT	-----	-----MAEKQKHDGRV	KIGHYILGD	TLGVGT	FGK	30
Q13131	AAPK1_HUMAN	-----	-----MATAEKQKHDGRV	KIGHYILGD	TLGVGT	FGK	32
Q5EG47	AAPK1_MOUSE	-----	-----MAEKQKHDGRV	KIGHYILGD	TLGVGT	FGK	30
Q5U118	Q5U118_DROME	-----	-----MPQMRAAA	EVAAGSANGQPLV	KIGHYLLGAT	TLGTGTFGK	41
Q95ZQ4	AAPK2_CAEL	RKDRD	STDNSSKMS	SPGGETSTKQ	QQLKAQIKIGHY	ILKETLGVGT	100
P06782	SNF1_YEAST	HHHHHHHHHH	HGHGGSNSTL	NNPKSSLADGA	HIGNYQIVK	TLGEGSF	68
				: : * :	*** * : ** :		
Q9XYP6	Q9XYP6_DICDI	CHHHMV	VHRDLKPEN	LLLDP	PINKCIKIAD	FGLSNMQD	194
Q38997	KIN10_ARATH	CHRN	MVHRDLKPEN	LLDSK	-CNVKIAD	FGLSNIMRD	204
P54645	AAPK1_RAT	CHRHM	VHRDLKPEN	VLLDAH	-MNAKIAD	FGLSNMMSD	179
Q13131	AAPK1_HUMAN	CHRHM	VHRDLKPEN	VLLDAH	-MNAKIAD	FGLSNMMSD	181
Q5EG47	AAPK1_MOUSE	CHRHM	VHRDLKPEN	VLLDAH	-MNAKIAD	FGLSNMMSD	179
Q5U118	Q5U118_DROME	CHRHM	I	VHRDLKPEN	LLLDHN	-MHVKIAD	190
Q95ZQ4	AAPK2_CAEL	CHRHM	VHRDLKPEN	LLDEQ	-NNVKIAD	FGLSNIMTD	249
P06782	SNF1_YEAST	CHRHK	I	VHRDLKPEN	LLDEH	-LNVKIAD	206
		** : :	: ***** :	***	***** :	* ** . * : *****	
Q9XYP6	Q9XYP6_DICDI	YAAPEVIS	SGKLYAGPEVD	VW	SCGVILYAF	LCALPFD	244
Q38997	KIN10_ARATH	YAAPEVIS	SGKLYAGPEVD	VW	SCGVILYAL	LCGLPFD	254
P54645	AAPK1_RAT	YAAPEVIS	SGRLYAGPEVD	IW	SSGVILYAL	LCGLPFD	229
Q13131	AAPK1_HUMAN	YAAPEVIS	SGRLYAGPEVD	IW	SSGVILYAL	LCGLPFD	231
Q5EG47	AAPK1_MOUSE	YAAPEVIS	SGRLYAGPEVD	IW	SSGVILYAL	LCGLPFD	229
Q5U118	Q5U118_DROME	YAAPEVIS	SGKLYAGPEVD	IW	SCGVILYAL	LCGLPFD	240
Q95ZQ4	AAPK2_CAEL	YAAPEVIS	SGKLYAGPEVD	VW	SCGVILYAL	LCGLPFD	299
P06782	SNF1_YEAST	YAAPEVIS	SGKLYAGPEVD	VW	SCGVILYV	MLCRRLPFD	256
		***** :	***** :	** . ***** :	**	***** : : * ** : *	

(B)

Figure 1. (A). The plasmid map of genomic region encompassing AMPK α subunit (*Chromosome 3* coordinates 589784–592434, Watson strand) (*DictyBase* <http://dictybase.org>) cloned into pZEr₀₂. The AMPK α subunit in *Dictyostelium* is encoded by a 2.6kb gene. (B). The AMPK α subunit amino acids sequences of *Dictyostelium discoideum* using CLUSTAL W sequence alignment program (<http://expasy.org>) showed 61% homology to mammalian cells (*Homo sapiens* and *Rattus norvegicus*), 56% to *Drosophila melanogaster*, 61% to *Ceanorhabditis elegans*, 65% to *Arabidopsis thaliana* and 64% to *Saccharomyces cerevisiae*. The N-terminus contains a highly conserved catalytic core, S₁TKc domain and identical APE (shaded blue) and DFG (shaded purple) motifs with other eukaryotic cells. The residue (tyrosine, Y) shaded pink is conserved and marks the start of the catalytic domain in all eukaryotes. The asterisk (*) means residues are identical in all sequences in the alignment. The colon (:) means conservative substitutions are present that is, residues are identical or replaced by amino acids with similar biochemical properties. The period (.) means partially conservative substitutions of similar amino acids. The residue asparagine (N) at position 166 is only present in *D. discoideum*. Residue numbers to the right of the figure. Each amino acid residue is represented with one letter code.

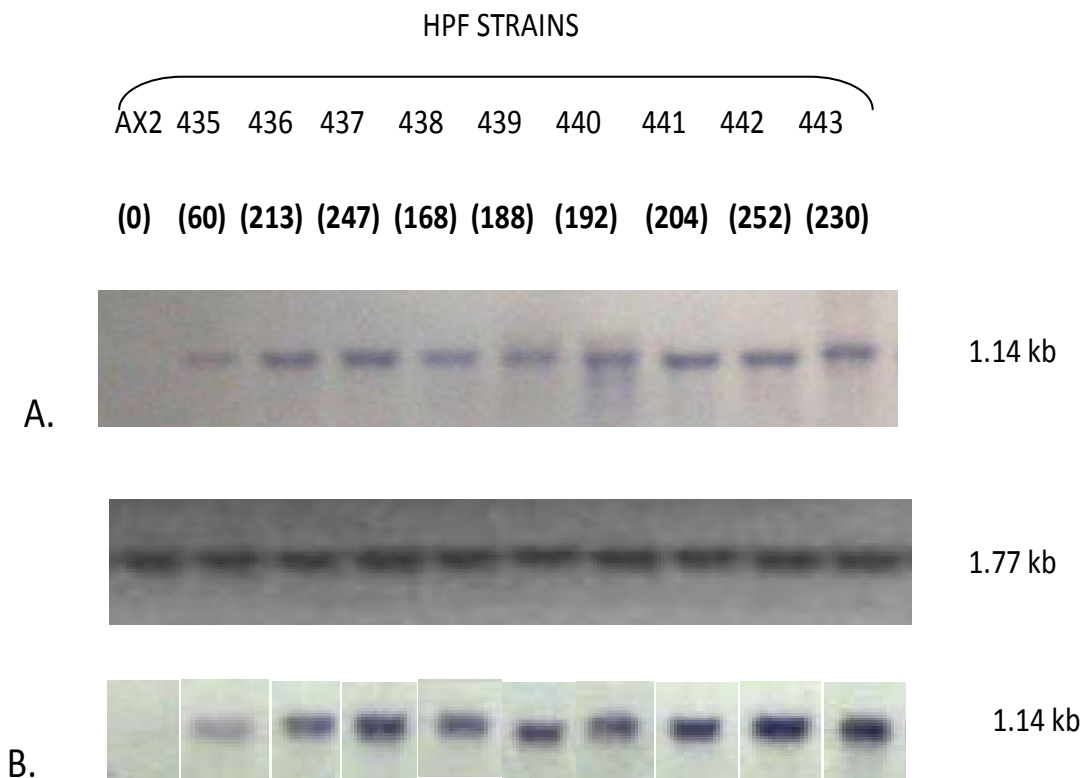


Figure 2. The plasmid copy number-dependent steady state RNA expression levels of the AMPK α subunit in overexpression strains. Genomic DNA and total RNA were extracted from stable transformants bearing plasmid expression vector construct (pPROF392) expressing the truncated catalytic domain of the AMPK α subunit (α^{380}). Figures atop the Southern blot indicate HPF strain identification number. Copy numbers for pPROF392 are indicated in parentheses. A) Genomic DNA from *D. discoideum* AX2 and overexpression strains (HPF434 – HPF442) were digested with *EcoRI* and subjected to electrophoresis on 1% agarose gel, blotted onto nylon membrane and probed with DIG-labelled AMPK α subunit DNA fragment. The different bands (1.14 kb) showing different intensities represent each strain indicating there are variations in the copies of the overexpression plasmid construct (pPROF392) insertions in the genome. The lower panel shows same genomic DNA probed with GTP-binding protein (β subunit) probe (1.77 kb), served as indicator that similar concentrations of the genomic DNA were used per strain. B) Total RNA (1.14 kb) from corresponding strains were separated in a formaldehyde agarose gel, transferred onto nylon membrane and probed with DIG-labelled AMPK α subunit DNA. The blot shows RNA expression levels in the respective strains are closely related to the copy numbers. Endogenous transcript is not detectable with the probe in northern blot.

in mitochondrial mass is an indication of mitochondrial proliferation. In the same vein, the more severe the antisense inhibition, the more the apparent decrease in the Advanced Technology Program (ATP).

Effects of AMPK α subunit expression on ATP levels

Since mitochondrial biogenesis was stimulated in AMPK α^{380} overexpressing cells it is anticipated that ATP levels in these cells would be altered in a similar fashion. The ATP levels in AMPK α^{380} overexpression cells were significantly elevated in the range of 2 to 4 folds relative

to the ATP levels in AX2 strain (Figure 6). The higher the plasmid copies, the more the ATP production per cell. These findings are consistent with the role of AMPK in energy homeostasis and infer that AMPK activation in response to chronic energy stress boosts ATP generation to maintain energy expensive cellular functions. Conversely, the severe the antisense inhibition, the more apparent the ATP decrease. Taken together, this finding provides genetic evidence that AMPK plays a critical role in mitochondrial proliferation. Thus, constitutive AMPK activation initiates signalling pathways that would result in mitochondrial biogenesis. These findings show that constitutive activation of AMPK cause increase in mitochondrial

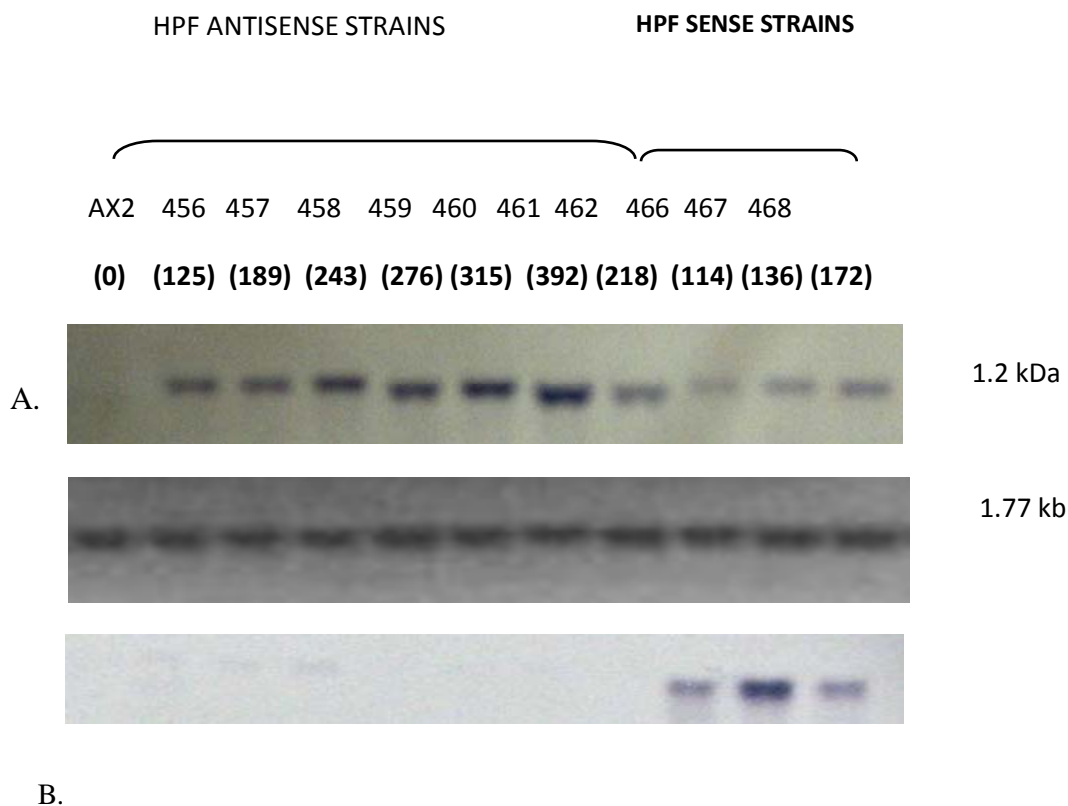


Figure 3. The plasmid copy number-dependent steady state RNA expression levels of the AMPK α subunit antisense plasmid construct in stable transformants evaluated by northern blotting. Genomic DNA and total RNA were extracted from stable transformants bearing plasmid expression vector constructs expressing the antisense RNA (pPROF362) complementary to part of the catalytic domain of the AMPK α subunit and the sense control strains. Figures atop the Southern blot indicate HPF strain identification number. Copy numbers pPROF362 are indicated in parenthesis. A) Genomic DNA from *D. discoideum* AX2 and antisense inhibited strains (HPF456 – HPF462) and complimentary sense strains (HPF466 – HPF468) were digested with *EcoRI* and subjected to electrophoresis on 1 % agarose gel, blotted onto nylon membrane and probed with DIG-labelled AMPK α subunit DNA fragment. The different bands showing varying intensities for each strain indicate there are variations in the copies of the antisense plasmid construct (pPROF362) and the control sense plasmid construct (pPROF361) insertions in the genome. The lower panel shows the same genomic DNA probed with GTP-binding protein (β subunit) probe, served as indicator that similar concentrations of the genomic DNA were used per strain. B) Total RNA from respective strains were separated in formaldehyde agarose gel, transferred onto nylon membrane and probed with DIG-labelled AMPK α subunit DNA. The blot shows RNA expression levels in the respective strains are closely related to the copy numbers. Endogenous transcript is not detectable with the probe in northern blot.

mitochondrial content in *D. discoideum*. This constitutes direct evidence that genetic activation of AMPK culminates in mitochondrial biogenesis.

DISCUSSION

AMPK has been the focus of increasing attention for its fundamental roles in cellular energy homeostasis in healthy cells and in a variety of pathological situations,

most notably diabetes, cancer (Hardie and Hawley, 2001; Winder and Hardie, 1999) and mitochondrial diseases (Bokko et al., 2007). Healthy cells AMPK, a heterotrimeric complex comprising of a catalytic α subunit (Crute et al., 1998), regulatory non-catalytic β (Thornton et al., 1998), and γ subunits (Carling et al., 1994), is activated very sensitively by stresses such as strenuous exercise, ischaemia or glucose deprivation (Salt et al., 1998). ATP hydrolysis yields ADP that helps replenish cellular ATP by donating a phosphate group to another ADP, forming

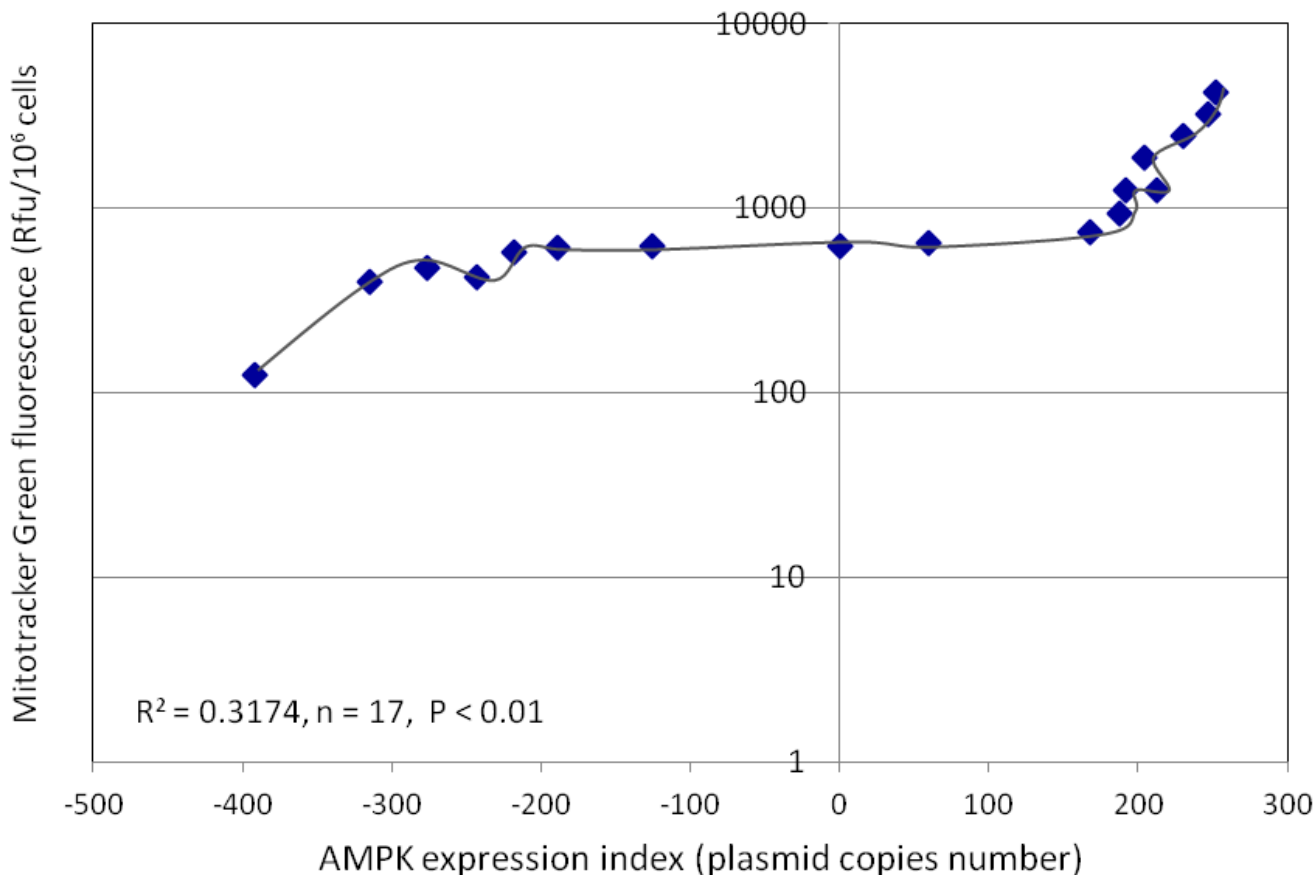


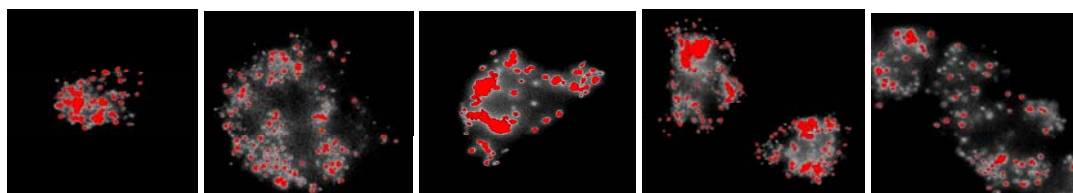
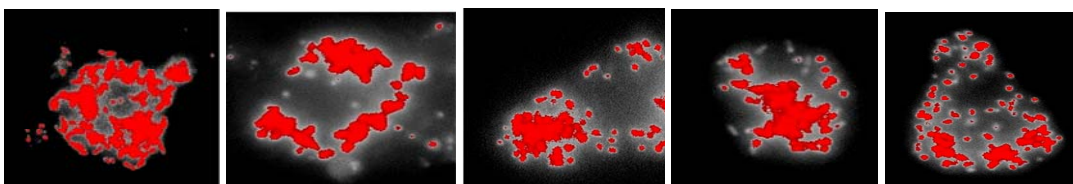
Figure 4. Effect of AMPK α subunit expression on mitochondrial mass in *Dictyostelium*. Mitochondrial “mass” was measured by fluorescence with the mitochondrion-specific dye, Mitotracker Green after subtraction of autofluorescence from unstained cells and presented as relative fluorescence units per 10^6 cells. The blue circles with red borders represent individual strains each carrying the indicated number of copies of the AMPK α^{380} overexpression construct while gray circles stand for strains each carrying the indicated number of copies of AMPK α subunit antisense construct. Each red square represents a strain carrying both the chaperonin 60 antisense construct and the AMPK α antisense construct per genome. The dark blue circles represent the AX2, the wild type parental strain used as control. Compared to wild type cells, the Mitotracker Green fluorescence was higher in the case of AMPK α^{380} overexpression, but reduced in the AMPK α subunit antisense-inhibited strain cells. R^2 is the coefficient of variation and equals the square of the Pearson product-moment correlation coefficient. The significance probability is the probability of the observed results occurring under the null hypothesis that the correlation coefficient was zero. Negative values indicate the copy numbers of the AMPK α subunit antisense inhibition construct, while positive values indicate copy numbers of the overexpression construct.

an ATP and an AMP. The dramatic rise of AMP: ATP ratio leads to an activation of AMPK via allosteric activation (Adams et al., 2004; Scott et al., 2004) and phosphorylation by AMPK-kinase (AMPKK) (Weekes et al., 1994; Hawley et al., 1995; Stein et al., 2000) allowing ≥ 200 -fold activity. Thus, AMPK functions as a metabolic master switch, or more accurately, ‘low fuel warning system’ in mammalian (Winder and Hardie, 1999; Hardie and Hawley, 2001) and other eukaryotic cells (Wilson et al., 1996; Carlson, 1999; Pan and Hardie, 2002). The activated cascade regulates metabolic pathways and promotes the adaptation of eukaryotic cells to their micro-environment in response to the ever changing energy

charge (Hardie and Hawley, 2001; Suzuki et al., 2007). This, places AMPK holoenzyme at a central control point in maintaining cellular energy homeostasis. This pivotal role places AMPK in an ideal position to also play a wider role in regulating whole-body energy metabolism (Carling, 2004).

Given that all physiological processes depend on energy supply in the form of ATP, there are potentially many links with AMPK. Rapid progress in the field has also created great expectations that AMPK will be an important therapeutic target for the treatment of diabetes, obesity, cancer, cardiovascular disease and mitochondrial diseases. Irrespective of these outcomes,

A: AX2: Wild type cells

B: AMPK α^{380} 

C: Antisense inhibited strains

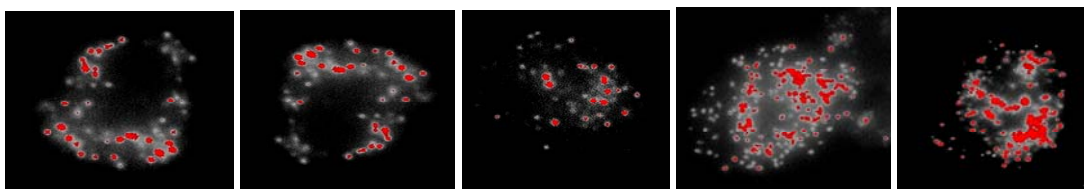


Figure 5. Mitotracker Red fluorescence microscopy of representative AMPK overexpressing, AMPK antisense-inhibited strains and wild type cells. Vegetative cells from AX2, AMPK α^{380} overexpressing and AMPK α antisense-inhibited strains were stained with the mitochondrion-specific dye, Mitotracker Red and analysed by fluorescence microscopy. Compared to wild type cells (panel A), the Mitotracker Red fluorescence was more intense in the cells from AMPK α^{380} overexpression strains (panel B), but similar to the AMPK α antisense-inhibited cells (panel C).

we can be assured that AMPK research will provide many new insights into the integration of metabolism and physiological functions. Despite the complexities of energy metabolism, it is clear that the primary trigger for mitochondrial biogenesis is an inability of the mitochondria to produce energy in the form of ATP to match the corporal demand. Constitutive activation of AMPK approximates the persistent AMPK activation such as from stresses. The strains expressing AMPK α^{380} had varied but stable plasmid copies of the plasmid construct and corresponding varied levels of RNA expression. The strains expressing the constitutively active *Dictyostelium* AMPK α^{380} phenocopied the chronic activation of AMPK and exhibited increased expression of RNA manifolds the level in wild type cells.

Truncation of the mammalian AMPK α subunit catalytic domain created a constitutively active form of AMPK and expression was characterised by significant increase in activity of the AMPK (Crute et al., 1998). The constitutively active AMPK has also shown to be resistant

to inactivation by protein phosphatase 2C (Woods et al., 2000). Strains expressing the antisense construct contained varied plasmid copies and corresponding RNA expression profile depicting diminution of RNA as the plasmid copies increased. Antisense inhibition of the AMPK α subunit led to significant reduction of expression and consequently attenuation of AMPK function. This indicates degradation in the antisense RNA expressing transformants of both the antisense and the native mRNA. This would mean lower expression levels of the native mRNA. During successful antisense, RNA inhibition, both strands of the mRNA and antisense RNA duplex, are degraded by the RISC complex (Hinas and Söderbom, 2007). Earlier attempts at creating a knockout strain or antisense inhibited strains with plasmid copies higher than 400, which were not successful. This possibly shows that strains in which APMK is knocked out may not be viable. Additionally, strains with severely attenuated RNA expression beyond a particular threshold may also not survive. Moreover, strains with higher plasmid copies

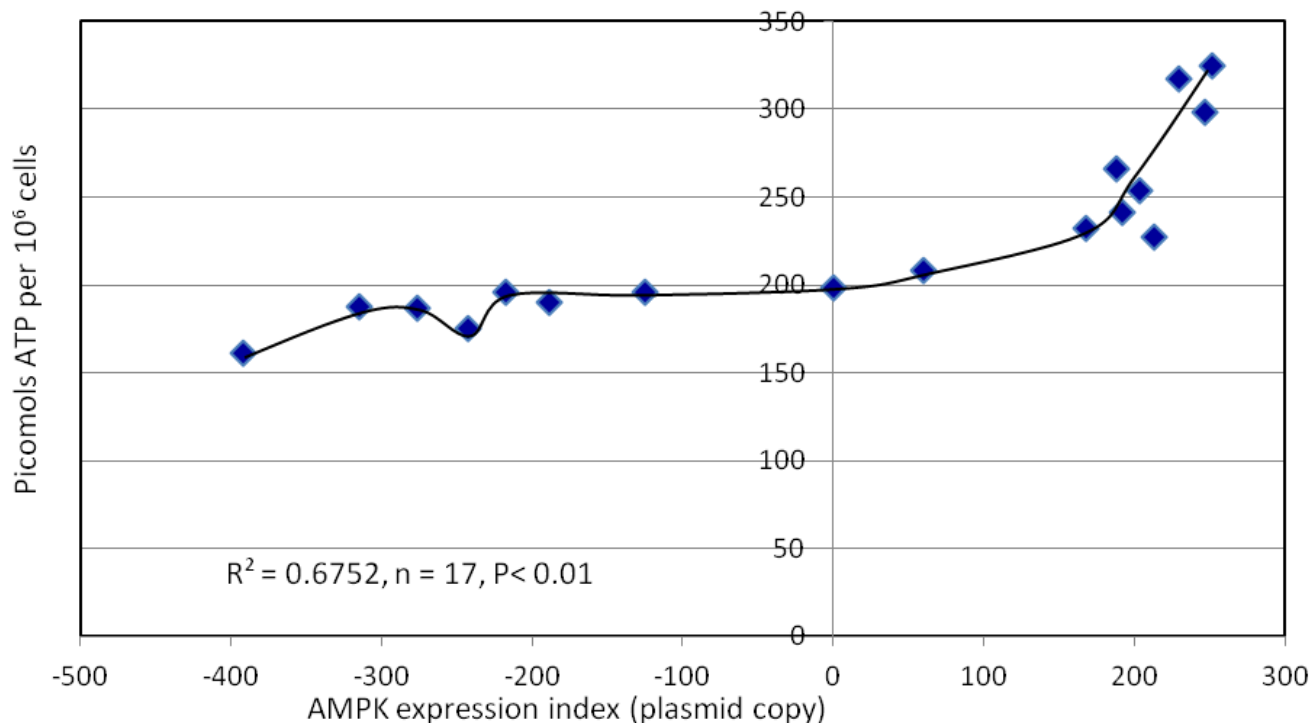


Figure 6. Effect of AMPK α subunit expression on ATP levels in *Dictyostelium*. ATP levels in *Dictyostelium* cells was measured using luciferase-based luminescence in a Turner Modulus Fluorometer with the luminescence module and presented as picomoles per 10^6 cells. The gray circles represent strains carrying the indicated number of copies of an AMPK α subunit antisense construct while the blue circles represents strains carrying the indicated number of copies of the AMPK α^{380} overexpression construct per genome. Each red square represents a different strain carrying both the AMPK α antisense construct and the chaperonin 60 antisense construct. The black circle represents AX2, the wild type parental strain used as control. R^2 is the coefficient of variation and equals the square of the Pearson product-moment correlation coefficient. The significance probability is the probability of the observed results occurring under the null hypothesis that the correlation coefficient was zero. Negative values indicate the copy numbers of the AMPK α antisense inhibition constructs, while positive values indicate copy numbers of the overexpression construct used as expression indices.

of antisense plasmids showed severe growth and development defects (Bokko et al., 2007).

Overexpression of a constitutively active form of the AMPK α subunit resulted in increased mitochondrial content, mitochondrial mass and ATP levels. The mitochondrial dyes (Mitotracker Red and Mitotracker Green) showed that AMPK α^{380} overexpression resulted in increased mitochondrial mass in *Dictyostelium* cells indicative of mitochondrial proliferation. By constitutive activation of AMPK, mitochondrial dysfunction can be countervailed to generate energy. As in human cells, AMPK in *Dictyostelium* stimulates the proliferation of mitochondria and elevated ATP production. This finding corroborates Williams et al. (1986) and Zong et al. (2002) who reported that in mammalian cells, particularly in muscle tissues, AMPK activity leads to mitochondrial proliferation. Indeed, Zong et al. (2002) stated that AMPK is the proximal signalling step in stimulation of mitochondrial biogenesis in mammalian cells. This is part of the

response to strenuous physical training in athletes and is a component of AMPK's roles in energy homeostasis in healthy cells. Prolonged AMPK activation essentially sequel to mitochondrial dysfunction initiates mitochondrial biogenesis to buffer energy deficits and low ATP level in the cell in response to chronic energy deprivation. Thus, by sensing the energy status of the cell, AMPK initiates events culminating in mitochondrial biogenesis. Genetic activation of AMPK mimics activation, culminating in mitochondrial proliferation. Furthermore, the ATP levels were elevated in AMPK α subunit overexpression strains sequel to mitochondrial proliferation. This work adds to the multiple machinery channels that concertedly culminate in mitochondrial biogenesis.

Conversely, antisense inhibition of AMPK α subunit did not significantly affect mitochondrial content or ATP levels at lower plasmid copies. The ATP levels and mitochondrial content were similar to the wild type strain. As the functional attenuation by antisense inhibition becomes

severe, the mitochondrial content and ATP level diminution becomes apparent. For instance, strain HPF461 with the highest plasmid copies, had the least fluorescence when stained with mitotracker green as well as lowest ATP level. Antisense strains may establish new energy threshold in the strains or had inapparent effect on AMPK activity with respect to mitochondrial content. Earlier reports suggested that mitochondria may undergo fusion with other mitochondria or become inactive when the energy use is low (Hermann et al., 1998; Chan, 2006). Furthermore, Jones et al. (2012) advocated that mitochondria alter their function according to prevailing cellular energetic requirements and thus function as sensors that generate signals to adjust fundamental cellular processes through a retrograde mitochondria-nucleus signalling pathway.

Conclusion

Taken together, this work show that AMPK plays a critical role in mitochondrial proliferation. Constitutive activation of AMPK initiates signalling to downstream targets pathways that culminates in increased mitochondrial mass in *D. discoideum*. This constitutes direct evidence that genetic activation of AMPK propels *in vivo* mitochondrial biogenesis and ATP generation in *D. discoideum*.

ACKNOWLEDGEMENTS

We gratefully acknowledge the support of La Trobe University Postgraduate Research Scholarship (LTUPRS) and the Australian Government International Postgraduate Research Scholarship Scheme (IPRSS) without which the present study could not have been completed.

Conflict of interest

Authors declare that there are no conflicts of interests

REFERENCES

- Adams J, Chen ZP, Van Denderen BJ, Morton CJ, Parker MW, Witters LA, Stapleton D, Kemp BE (2004). Intracellular control of AMPK via the γ_1 subunit AMP allosteric regulatory site. *J. Environ. Prot. Sci.* 13:155-165.
- Ausubel FM, Albright LM (1995). Molecular Techniques and Gene Cloning. In: Ausubel FM, Brent R, Kingston RE, Moore D, Seidman JG, Smith JA, Struhl K (Eds.), *Current Protocols in Molecular Biology*. John Wiley New York, USA. pp. 337-525.
- Bergeron R, Ren JM, Cadman KS, Moore IK, Perret P, Pypaert M, Young LH, Semenkovich CF, Shulman GI (2001). Chronic activation of AMP kinase results in NRF-1 activation and mitochondrial biogenesis. *Am. J. Physiol. Endocrinol. Metab.* 281: E1340-E1346.
- Black BL, Olson EN (1998). Transcriptional control of muscle development by myocyte enhancer factor-2 (MEF2) proteins. *Ann. Rev. Cell. Dev. Biol.* 14: 167-196.
- Bokko BP Said F, Bandala E, Ahmed A, Annesely SJ, Huang X, Khurana T, Kimmel AR, Fisher PR (2007). Diverse cytopathologies in mitochondrial disease are caused by AMPK. *J. Mol. Cell Biol.* 18: 1874-1886.
- Carling D (2004). The AMP-activated protein kinase cascade—a unifying system for energy control. *Trends Biochem. Sci.* 29: 18-24.
- Carling D, Aguan K, Woods A, Verhoeven AJM, Beri RK, Brennan CH, Sidebottom C, Davison MD, Scott J (1994). Mammalian AMP-activated protein kinase is homologous to yeast and plant protein kinases involved in the regulation of carbon metabolism. *J. Biol. Chem.* 269: 11442-11448.
- Carlson M (1999). Glucose repression in yeast. *Curr. Opin. Microbiol.* 2: 202-207.
- Chan DC (2006). "Mitochondria: Dynamic Organelles in Disease, Aging, and Development". *Cell* 125(7):1241-1252.
- Clayton DA (1992). Transcription and replication of animal mitochondrial DNAs. *Int. Rev. Cytol.* 141:217-232.
- Corton JM, Gillepsie JG, Hawley SA, Hardie DG (1995). 5'-Aminoimidazole-4-carboxamide ribonucleoside. A specific method for activating AMP-activated protein kinase in intact cells? *Eur. J. Biochem.* 229:558-565.
- Crute BE, Seefeld K, Gamble J, Kemp BE, Witters LA (1998). Functional domains of the α_1 catalytic subunit of the AMP-activated protein kinase. *J. Biol. Chem.* 273:35347-35354.
- Czubryt MP, McAnally J, Fishman GI, Olson EN (2003). Regulation of peroxisome proliferator-activated receptor γ coactivator 1 α (PGC-1 α) and mitochondrial function by MEF2 and HDAC5. *Proc. Natl. Acad. Sci.* 100:1711-1716.
- Fey P, Compton K, Cox E (1995). Green fluorescent protein production in the cellular slime molds *Polysphondylium pallidum* and *Dictyostelium*. *Gene* 165:127-130.
- Goffart S, von Kleist-Retzow JC, Wiesner RJ (2004). Regulation of mitochondrial proliferation in the heart: power-plant failure contributes to cardiac failure in hypertrophy. *Cardiovasc. Res.* 64: 198-207.
- Grozinger CM, Schreiber SL (2000). Regulation of histone deacetylase 4 and 5 and transcriptional activity by 14-3-3-dependent cellular localization. *Proc. Natl. Acad. Sci.* 97:7835-7840.
- Gulick T, Cresci S, Caira T, Moore DD, Kelly DP (1994). The peroxisome proliferator activated receptor regulates mitochondrial fatty acid oxidative enzyme gene expression. *Proc. Natl. Acad. Sci.* 91:11012-11016.
- Hardie DG, Hawley SA (2001). "AMP-activated protein kinase: the energy charge hypothesis revisited". *Bioessays* 23:1112-1119.
- Hawley SA, Selbert MA, Goldstein EG, Edelman AM, Carling D, Hardie DG (1995). 5'-AMP activates the AMP-activated protein kinase cascade, and Ca²⁺/calmodulin the calmodulin-dependent protein kinase I cascade, via three independent mechanisms. *J. Biol. Chem.* 270:27186-27191.
- Hayashi T, Hirshman MF, Fujii N, Habinowski SA, Witters LA, Goodyear LJ (2000). Metabolic stress and altered glucose transport: activation of AMP-activated protein kinase as a unifying coupling mechanism. *Diabetes* 49:527-531.
- Hermann GJ, Thatcher JW, Mills JP, Hales KG, Fuller MT, Nunnari J, Shaw JM (1998). "Mitochondrial Fusion in Yeast Requires the Transmembrane GTPase Fzo1p". *J. Cell. Biol.* 143(2):359-373.
- Hermann JM, Neupert W (2000). "Protein transport into mitochondria". *Curr. Opin. Microbiol.* 3(2):210-214.
- Hinas A, Söderbom F (2007). Treasure hunt in an amoeba: non-coding RNAs in *Dictyostelium discoideum*. *Curr. Genet.* 51:141-159.
- Ihlemann J, Ploug T, Hellsten Y, Galbo H (1999). Effect of tension on contraction-induced glucose transport in rat skeletal muscle. *Am. J. Physiol. Endocrinol. Metab.* 277:E208-E214.
- Jones AWE, Yao Z, Vicencio JM, Karkucinska-Wieckowska A, Szabadkai G (2012). PGC-1 family coactivators and cell fate: Roles

- in cancer, neurodegeneration, cardiovascular disease and retrograde mitochondria–nucleus signalling. *Mitochondrion* 12:86–99.
- Lehman JJ, Barger PM, Kovacs A, Saffitz JE, Medeiros DM, Kelly DP (2000). Peroxisome proliferator-activated receptor γ coactivator-1 promotes cardiac mitochondrial biogenesis. *J. Clin. Investig.* 106(7):847–856.
- Lehman JJ, Kelly DP (2002). Transcriptional activation of energy metabolic switches in the developing and hypertrophied heart. *Clin. Exp. Pharmacol. Physiol.* 29: 339–345.
- Lin J, Wu H, Tarr PT, Zhang CY, Wu Z, Boss O, Michael LF, Puigserver P, Isotani E, Olson EN, Lowell BB, Bassel-Duby R, Spiegelman BM (2002). Transcriptional co-activator PGC-1 α drives the formation of slow-twitch muscle fibres. *Nature* 418:797–801.
- Liu Y, Wan Q, Guan Q, Gao L, Zhao J (2006). High-fat diet feeding impairs both the expression and activity of AMPK α in rats' skeletal muscle. *Biochem. Biophys. Res. Commun.* 339:701–707.
- McKinsey TA, Zhang CL, Olson EN (2001). Identification of a signal-responsive nuclear export sequence in class II histone deacetylases. *Mol. Cell Biol.* 21:6312–6321.
- Michael LF, Wu Z, Cheatham RB, Puigserver P, Adelmant G, Lehman JJ, Kelly DP, Spiegelman BM (2001). Restoration of insulin-sensitive glucose transporter (GLUT4) gene expression in muscle cells by the transcriptional coactivator PGC-1. *Proc. Natl. Acad. Sci.* 98:3820–3825.
- Nellen W, Silan C, Firtel RA (1984). DNA-mediated transformation in *Dictyostelium discoideum*: Regulated expression of an actin gene fusion. *Mol. Cell Biol.* 4:2890–2898.
- Nisoli E, Clement E, Paolucci C, Cozzi V, Tonello C, Sciorati C, Bracale R, Valerio A, Francolini M, Moncada AS, Carruba MO (2003). Mitochondrial biogenesis in mammals: the role of endogenous nitric oxide. *Science* 299:896–899.
- Pan DA, Hardie DG (2002). A homologue of AMP-activated protein kinase in *Drosophila melanogaster* is sensitive to AMP and is activated by ATP depletion. *Biochem. J.* 367:179–186.
- Puigserver P, Wu Z, Park CW, Graves R, Wright M, Spiegelman BM (1998). A cold-inducible coactivator of nuclear receptors linked to adaptive thermogenesis. *Cell* 92:829–839.
- Reznick RM, Shulman GI (2006). The role of AMP-activated protein kinase in mitochondrial biogenesis. *J. Physiol.* 574(1):33–39.
- Salt IP, Celler JW, Hawley SA, Prescott A, Woods A, Carling D, Hardie DG (1998). AMP-activated protein kinase - greater AMP dependence, and preferential nuclear localization, of complexes containing the $\alpha 2$ isoform. *Biochem. J.* 334:177–187.
- Scarpulla RC, Vega RB, Kelly DP (2012). Transcriptional integration of mitochondrial biogenesis. *Trends Endocrinol. Metab.* 23(9):459–466.
- Scott JW, Hawley SA, Green KA, Anis M, Stewart G, Scullion GA, Norman DG, Hardie DG (2004). CBS domains form energy-sensing modules whose binding of adenosine ligands is disrupted by disease mutations. *J. Clin. Invest.* 113:274–284.
- Stein SC, Woods A, Jones NA, Davison MD, Carling D (2000). The regulation of AMP-activated protein kinase by phosphorylation. *Biochem. J.* 345:437–443.
- Sung S, Bisson S, Koehler S, Podgorski GJ (1999). The *Dictyostelium* Snf1/AMP-activated kinase. Unpublished. EMBL/GenBank ID AF118151.
- Suzuki A, Okamoto S, Lee S, Saito K, Shiuchi T, Minokoshi Y (2007). Leptin stimulates fatty acid oxidation and peroxisome proliferator-activated receptor α gene expression in mouse C2C12 myoblasts by changing the subcellular localization of the $\alpha 2$ form of AMP-activated protein kinase. *J. Mol. Cell Biol.* 27:4317–4327.
- Thornton C, Snowden MA, Carling D (1998). Identification of a novel AMP-activated protein kinase β subunit isoform which is highly expressed in the skeletal muscle. *J. Biol. Chem.* 273:12443–12450.
- Vega RB, Huss JM, Kelly DP (2000). The coactivator PGC-1 cooperates with peroxisome proliferator-activated receptor α in transcriptional control of nuclear genes encoding mitochondrial fatty acid oxidation enzymes. *Mol. Cell Biol.* 20:1868–1876.
- Ventura-Clapier R, Garnier A, Veksler V (2008). Transcriptional control of mitochondrial biogenesis: the central role of PGC-1 α . *Cardiovasc. Res.* 79:208–217.
- Wackerhage H, Woods NM (2002). Exercise-induced signal transduction and gene regulation in skeletal muscle. *J. Sports Sci. Med.* 1:103–114.
- Watts DJ, Ashworth JM (1970). Growth of myxameobae of the cellular slime mould *Dictyostelium discoideum* in axenic culture. *Biochem. J.* 119:171–174.
- Weekes J, Hawley SA, Corton J, Shugar D, Hardie DG (1994). Activation of rat liver AMP-activated protein kinase by kinase kinase in a purified, reconstituted system. Effects of AMP and AMP analogues. *Eur. J. Biochem.* 219:751–757.
- Williams RS, Salmons S, Newsholme EA, Kaufman RE, Mellor J (1986). Regulation of nuclear and mitochondrial gene expression by contractile activity in skeletal muscle. *J. Biol. Chem.* 261:376–380.
- Wilson WA, Hawley SA, Hardie DG (1996). The mechanism of glucose repression/derepression in yeast: SNF1 protein kinase is activated by phosphorylation under derepressing conditions, and this correlates with a high AMP:ATP ratio. *Curr. Biol.* 6:1426–1434.
- Winder WW, Hardie DG (1999). "AMP-activated protein kinase, a metabolic master switch: possible roles in type 2 diabetes". *Am. J. Physiol.* 277(1):E1–10.
- Winder WW, Holmes BF, Rubink DS, Jensen EB, Chen M, Holloszy JO (2000). "Activation of AMP-activated protein kinase increases mitochondrial enzymes in skeletal muscle". *J. Appl. Physiol.* 88(6):2219–2226.
- Witke W, Nellen W, Noegel A (1987). Homologous recombination in the *Dictyostelium* α -actin gene leads to an altered mRNA and lack of the protein. *EMBO J.* 6:4143–4148.
- Woods A, Azzout-Marniche D, Foretz M, Stein SC, Lemarchand P, Ferre P, Foulfelle F, Carling D (2000). Characterisation of the Role of AMP-Activated Protein Kinase in the Regulation of Glucose-Activated Gene Expression Using Constitutively Active and Dominant Negative Forms of the Kinase. *Mol. Cell Biol.* 20(18):6704–6711.
- Wu H, Kanatous SB, Thurmond FA, Gallardo T, Isotani E, Bassel-Duby R, Williams RS (2002). Regulation of Mitochondrial Biogenesis in Skeletal Muscle by CaMK. *Science* 296:349–352.
- Wu Z, Puigserver P, Andersson U, Zhang C, Adelmant G, Mootha V, Troy A, Cinti S, Lowell B, Scarpulla RC, Spiegelman BM (1999). Mechanisms controlling mitochondrial biogenesis and respiration through the thermogenic coactivator PGC-1. *Cell* 98: 115–124.
- Xia Y, Buja LM, Scarpulla RC, McMillin JB (1997). Electrical stimulation of neonatal cardiomyocytes results in the sequential activation of nuclear genes governing mitochondrial proliferation and differentiation. *Proc. Natl. Acad. Sci.* 94:11399–11404.
- Zong H, Ren JM, Young LH, Pypaert M, Mu J, Birnbaum MJ, Shulman GI (2002). AMP kinase is required for mitochondrial biogenesis in skeletal muscle in response to chronic energy deprivation. *Proc. Natl. Acad. Sci.* 99:15983–15987.